Charge Transmission Through A Single Molecule

A Density Matrix Approach

BACHELORARBEIT

zur Erlangung des akademischen Grades
Bachelor of Science
(B. Sc.)
im Fach Physik

eingereicht an der
Mathematisch-Naturwissenschaftlichen Fakultät I
Institut für Physik
Humboldt-Universität zu Berlin

von
Florian Klimm
geboren am 3.5.1989 in Leipzig

Betreuung:

1. *PD Dr. Volkhard May*
2. *Prof. Dr. Beate Röder*

eingereicht am: *30. September 2011*

Contents

1. Introduction

The progressing miniaturization of electronic components raises the question of the lower border for such basic functional units. Since molecules are smallest stable structures it is the final goal to shrink e.g. transistors, resistors and switches to such a level. This highlights the importance of the construction and theoretical description of single molecules attached by nano-electrodes under connection of voltage. The amount and temporal shape of the occurring current is of main interest.
In the last years it became possible to connect single molecules with scanning tunneling microscope (STM) and measure current-voltage-(IV)-characteristics. Experiments mainly focus on organic molecules, especially polymers like phthalocyanines.
Of further interest is the controlling and switching of such molecular junctions. A change of the current flow can be achieved by the coupling to an external laser pulse, which enables the charge transmission through excited electronic states.
The dependence of current to voltage is macroscopic understood by Ohm[1]'s Law for about 200 years [1]. Nevertheless by investigating the behavior in microscopic scales the simple dependency fails and currently there is no consistent theory to describe such processes. There are a wide range of techniques to describe the charge flow through single molecules, e.g. Green functions, density matrix approach, rate equations and scattering theory.
In own calculations [2] of steady-state currents with the rate equation theory it was shown that in the absence of intramolecular vibrational redistribution (IVR) the photoswitching is hardly practicable. An adequate description within the reduced density matrix theory of the charge transmission through single molecules including optical excitation was presented in [3]. Thereby the IV-characteristics were calculated and discussed. Recent calculations [4] showed that the photoswitching of molecules can described by reducing the just mentioned density matrix approach to rate equations. This analysis contained the time-dependent current-switching behavior with photo-excitation by a laser pulse.
We want to continue this work by not reducing the density matrix approach to rate equations, but calculating the time-evolution of the whole reduced density matrix. The resulting differential equations were solved numerically with the VODE-algorithm.
Firstly we calculated the steady-state currents for the IV-characteristics with and without photoexcitation. Additionally the transient behavior of the molecule while excited by Gaussian-shaped laser pulses is shown. Furthermore we investigate the importance of IVR and show that small molecule-lead-couplings prohibit an efficient current switch.

[1] Georg Simon Ohm (1789-1854), Germany

2. Theoretical description

2.1 Hamiltonian of a molecule

The Hamiltonian[1] of a molecule H_{mol} can be expressed as

$$H_{mol} = H_{nuc} + H_{el} = T_{nuc} + T_{el} + V_{nuc} + V_{el} + V_{el-nuc} \ , \tag{2.1}$$

whereas T_i are the kinetic energies of the nuclei and the electrons. Spin-orbit coupling as well as relativistic effects are ignored. Coulomb [2] forces are described with the attraction potentials between each nucleus and electron V_{el-nuc} and the repulsing ones between particles of the same kind by V_{nuc} and V_{el}. The solutions of the time-independent Schrödinger[3] equation are the eigenstates and will be refered as the molecule wave functions $\psi(r, R, \sigma)$ which are dependent on the spatial coordinates of the electrons r and of the nuclei R as well as on the spins σ

$$H_{mol}\psi(r, R, \sigma) = \epsilon\psi(r, R, \sigma). \tag{2.2}$$

The eigenvalues ϵ are the energies of the molecule and in general there will exist a spectrum of eigenvalues ϵ_λ and associated eigenfunctions ψ_λ. We will name the lowest energy level ϵ_0 the ground-state energy. Due to the fact that the Hamiltonian does not react on the spin the wavefunction can be divided and in the following we will refer only to the spatial part

$$\psi(r, R, \sigma) = \psi(r, R)\Sigma(\sigma) \ , \tag{2.3}$$

2.1.1 Born-Oppenheimer Separation

Since (2.1) is often not exact solvable[4] and numerical calculation of polyatomic molecules needs a huge effort, an approximation is necessary. Born[5] and Oppenheimer[6] published in 1927 a method to separate the electronic and nuclear wavefunctions by referring to the large mass difference of the electrons and the nuclei of $\frac{m_{el}}{m_n} < 10^{-3}$. The picture of an

[1] Sir William Hamilton (1805-1865), Ireland
[2] Charles Augustin de Coulomb (1736-1806), France
[3] Erwin Schrödinger (1887-1961), Germany
[4] even the simplest molecule, the Hydrogenium-ion H_2^+ is not exact solvable [5]
[5] Max Born (1882-1970), Germany
[6] Julius Robert Oppenheimer (1904-1967), USA

instant reaction of the electron wave functions on nuclear changes allows us to define the electronic Hamiltonian

$$H_{el}(R) = T_{el} + V_{el-nuc} + V_{el-el} \ , \tag{2.4}$$

with the eigenfunctions $\phi_a(r, R)$ and the eigenvalues $E_a(R)$

$$H_{el}(R)\phi_a(r, R) = E_a(R)\phi_a(r, R) \ , \tag{2.5}$$

and the important fact that the dependence on R is only in a parametrical way. The molecular wave functions can be described by an expansion with both the nuclear wave functions $\chi_a(R)$ and the *adiabatic* electronic wave functions $\phi_a(r, R)$

$$\psi(r, R,) = \sum_a \chi_a(R)_a\phi_a(r, R). \tag{2.6}$$

Inserting this expansion into the molecular Schrödinger equation (2.1) (ignoring the spin part) and taking into account that ϕ form a orthonormal basis ($\langle\phi_a|\phi_b\rangle = \delta_{ab}$) we gain an equation for the coefficients $\chi_a(R)$

$$(\underbrace{T_{nuc} + \underbrace{E_a + V_{nuc-nuc} + \Theta_{aa}}_{U_a}}_{H_a} - \epsilon)\chi_a(R) = -\sum_{a\neq b} \Theta_{ab}\chi_b(R) \ , \tag{2.7}$$

with the operator Θ_{ab} calculated in [6] and resulting of the action of the kinetical energy operator T_{nuc} on the states and are called nonadiabatic coupling. With (2.7) we received the exact Schrödinger equation for the nuclei movement with the effective potential U_a resulting in a *nuclear* or vibrational Hamiltonian H_a. The solution of (2.7) is $\chi_{a\mu}$ whereas the index μ refers to vibrational quantum numbers. Finally we receive the molecular wave function

$$\psi_\mu(r, R) = \sum_a \chi_{a\mu}(R)_a\phi_a(r, R). \tag{2.8}$$

2.1.2 Born-Oppenheimer Approximation

Keeping in mind the above mentioned large mass difference we may assume the nuclei to be clamped, i. e. their momentum is negligible. Within the *Born-Oppenheimer-Approximation* the nonadiabatic couplings Θ in (2.7), that are formed by the nuclear momentums, are ignored and $\Theta_{ab} = 0$ leads to

$$H_a\chi_{a\mu}(R) = \epsilon_{a\mu}\chi_{a\mu}(R). \tag{2.9}$$

The energetic spectrum $\epsilon_{a\mu}$ is formed by the electrical state, presented by the quantum number a and by the vibrational quantum number μ as well. Finally we receive the adiabatic wave function

$$\psi^{adia}_{a\mu}(r, R) = \chi_{a\mu}(R)\phi_a(r, R) \ , \tag{2.10}$$

which describes the total state of the molecule.

2.2 Potential Energy Surfaces

In (2.7) we introduced the effective potential U_a felt by the nuclei. It defines a hypersurface in the space of the nuclear coordinates on which all nuclear motions and reactions proceed. If N_{Nuc} is the number of nuclei the molecule is composed of, in general U_a is dependent on $3N_{Nuc}$ coordinates R_i. Due to the fact that translations in all 3 dimensions as well as rotations around all 3 solid axes do not affect the energy of the molecule only $3N_{Nuc} - 6$ coordinates are necessary for the complete description of the PES. The determination of the PES can be very challenging for large molecules. Fortunately often only a reduced number of coordinates is necessary, while the remaining may be fixed.
The PES of water H_2O in Fig. 2.1 is a function of 3 coordinates. But the limitation that both bonds have the same lengths r lead to a two dimensional PES with the angle between the hydrogen atoms Φ as second coordinate.
Important for state of the molecules are the *stationary points*. This are points in the phase space for which the gradient of the potential vanishes

$$\nabla U_a(R) = \left(\frac{\partial U_a}{\partial R_1}, ..., \frac{\partial U_a}{\partial R_{3N_{Nuc}}} \right) = 0 \, , \tag{2.11}$$

and the molecule may rest.
H_2O has two stationary constellations with both the bond length of $r = 0.9584\,\text{Å}$ and the angles $\Phi_1 = 104.45\,^\circ$ and $\Phi_2 = 255.55\,^\circ$. These are in fact the same situations since both ligands of the oxygen are hydrogen atoms.
Furthermore the PES allow us to analyze the dynamics of the molecule away from the stationary points, in general from one reactant well to a product well. Transitions may occur along different *reaction paths* on the multidimensional PES. The *minimum path* follows along the gradient (shallowest ascent/deepest descent) of potential energy from reactant to products and leads through the saddle point which is called *transition state*. The direct *rigid path* is disabled but may also be activated at higher energies. We will refer to the curves arc length along the (minimum) energy path as the one-dimensional *reaction coordinate*.

2.2.1 Harmonic Approximation

An important tool for the treatment of molecular dynamics in the proximity to the stationary points is the *harmonic approximation*. The Taylor[7] series of the PES $U_a(R)$ in a stationary point $R_0^{(a)}$ is given by

$$U_a(R) = U_a(R_0^{(a)}) + \underbrace{R\nabla U_a(R_0^{(a)})}_{=0} + \frac{1}{2} \sum_{n,m} \underbrace{\frac{\partial^2 U_a(R_0^{(a)})}{\partial R_m^{(a)} \partial R_n^{(a)}}}_{\kappa_{mn}} (R_n^{(a)} - R_n)(R_m^{(a)} - R_m) + O(R^3) \, , \tag{2.12}$$

at which we combined the partial second derivatives in the Hesse[8]-Matrix κ_{mn}. With the introduction of the *normal mode coordinates* $q_{a,\zeta}$ we transform the Hamiltonian of state a in a way that the Hesse matrix is diagonalized

[7] Brook Taylor (1685-1731), UK
[8] Otto Hesse (1811-1874), Germany

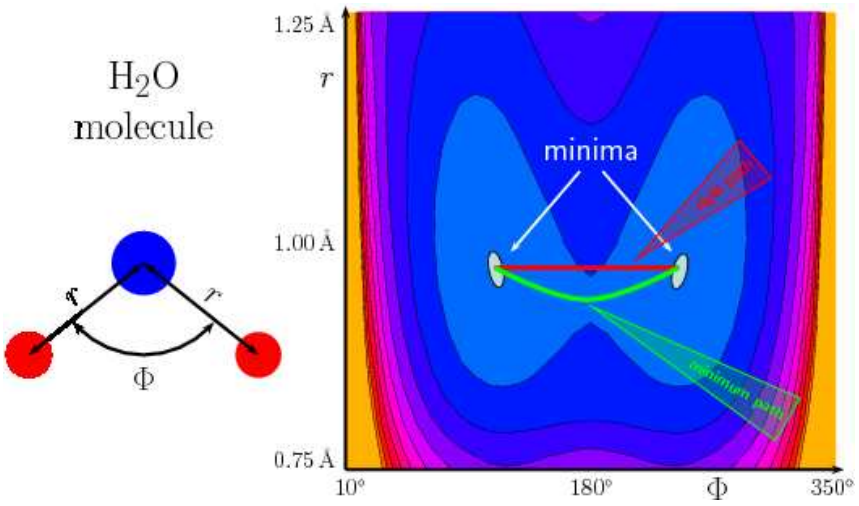

Figure 2.1: 2D Potential energy surface of H_2O as a function of the bond length r and the hydrogen angle Φ. The green arrow tip shows the transition state. After [7].

$$H_a = U_a(q_{a,\zeta} = 0) + \underbrace{\frac{1}{2}\sum_i \left(p_\zeta^2 + \omega_{a,\zeta}^2 q_{a,\zeta}^2\right)}_{H_a^{(nm)}}. \tag{2.13}$$

Hence the normal mode Hamiltonian $H_a^{(nm)}$ describes the harmonic vibration of the nuclei alongside the coordinates q_ζ with the frequencies ω_ζ. The problem of superposed harmonic oscillators is well understood and we receive the eigenenergies

$$E_{aN} = \sum_\zeta \hbar\omega_{a,\zeta}\left(N_\zeta + \frac{1}{2}\right). \tag{2.14}$$

The creation $C_\zeta^\dagger$ and annihilation operator C_ζ treating of the harmonic oscillator potential is common in literature (e.g. [6, 8]) and will be useful in the next section

$$q_\zeta = \sqrt{\frac{\hbar}{2\omega - \zeta}}\left(C_\zeta + C_\zeta^\dagger\right) \tag{2.15}$$

$$p_\zeta = -i\sqrt{\frac{\hbar\omega_\zeta}{2}}\left(C_\zeta + C_\zeta^\dagger\right) \tag{2.16}$$

$$H_a^{(nm)} = \sum_\zeta \hbar\omega_{a,\zeta}\left(C_\zeta^\dagger C_\zeta + \frac{1}{2}\right). \tag{2.17}$$

2.2.2 Franck-Condon-Factors

An important issue in molecular dynamics is the transition between different electronic states which are represented by shifted PES (Fig. 2.2). Such a transition from a *ground state* to the energetic higher *exited state* may be enabled by optical excitation. To simplify

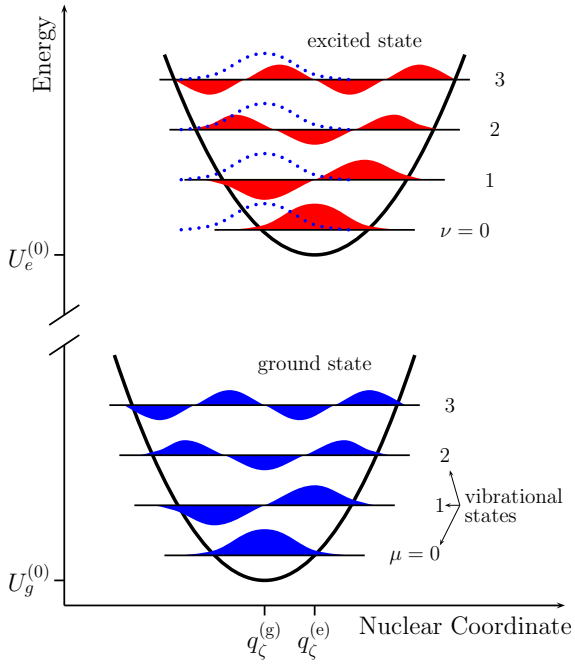

Figure 2.2: Two shifted harmonic oscillator PES with same ω and 4 lowest vibrational states drawn. FCF may be estimated by overlap of shifted ground state of vibrational level 0 (blue, dotted) and excited states (red, solid area): transition (g0) → (e1) is disabled, (g0) → (e0) and (g0) → (e3) are dominating.

matters we restrict our treatment to harmonic oscillator PES. Analog to (2.13) we may construct the Hamiltonian of a state that is shifted by $q_\zeta^{(a)}$ as

$$H_a = U_a(q_\zeta = q_\zeta^{(a)}) + \frac{1}{2}\sum_\zeta \left(p_\zeta^2 + \omega_{a,\zeta}^2 \left(q_\zeta - q_\zeta^{(a)}\right)^2\right) , \tag{2.18}$$

and may be transformed with the creation and annihilation operators to

$$H_a = U_a^{(0)} + \sum_\zeta \hbar\omega_\zeta \left(C_\zeta^\dagger C_\zeta + \frac{1}{2}\right) + \sum_\zeta \hbar\omega_\zeta \left(g_a(\zeta)\left(C_\zeta + C_\zeta^\dagger\right) + g_a^2(\zeta)\right) , \tag{2.19}$$

with the dimensionless shift of the PES

$$g_a(\zeta) = -\sqrt{\frac{\omega_\zeta}{2\hbar}} q_\zeta^{(a)} . \tag{2.20}$$

Below we will reduce the discussion to one single nuclear coordinate q. An important value for the transition rates from one vibronic state in the ground state $\chi_{a\mu}$ to another in the excited state $\chi_{b\nu}$ is the overlap of the wavefunktions $\langle\chi_{a\mu}|\chi_{b\nu}\rangle$ and are named the *Franck*[9]*-Condon*[10]*-Factors* (FCF). One way to calculate the FCF's via recursion formulas numerically is described in [6] and will be used below. We introduce the frequency quotient

$$\epsilon = \frac{\omega_b}{\omega_a} , \tag{2.21}$$

[9] James Franck (1882-1964), Germany
[10] Edward Condon (1902-1974), USA

and the dimensionless shift of the two PES towards each other

$$g = g_a - g_b \sqrt{\epsilon}\,. \tag{2.22}$$

The FCF can be calculated with the recursion relations

$$\langle \chi_{a\mu}|\chi_{b\nu}\rangle = \sqrt{\frac{\nu-1}{\nu}}\frac{1-\epsilon}{1+\epsilon}\langle \chi_{a\mu}|\chi_{b\nu-2}\rangle - \frac{2g\sqrt{\epsilon}}{\sqrt{\nu}(1+\epsilon)}\langle \chi_{a\mu}|\chi_{b\nu-1}\rangle + \sqrt{\frac{\mu\epsilon}{\nu}}\frac{2}{1+\epsilon}\langle \chi_{a\mu-1}|\chi_{b\nu-1}\rangle \tag{2.23}$$

$$\langle \chi_{a\mu}|\chi_{b\nu}\rangle = -\sqrt{\frac{\mu-1}{\mu}}\frac{1-\epsilon}{1+\epsilon}\langle \chi_{a\mu-2}|\chi_{b\nu}\rangle + \frac{2g}{\sqrt{\mu}(1+\epsilon)}\langle \chi_{a\mu-1}|\chi_{b\nu}\rangle + \sqrt{\frac{\nu\epsilon}{\mu}}\frac{2}{1+\epsilon}\langle \chi_{a\mu-1}|\chi_{b\nu-1}\rangle\,. \tag{2.24}$$

The initial value can be calculated to

$$\langle \chi_{a0}|\chi_{b0}\rangle = \frac{\sqrt{2\sqrt{\epsilon}}}{\sqrt{1+\epsilon}}\exp\left(-\frac{g^2}{1+\epsilon}\right), \tag{2.25}$$

which enables the calculation of all FCFs. Due to the negative exponential prefactor an increase of the PES's energy shift leads to a reduced overlap and hence to small transition rates. Note furthermore that in the often assumed case of $\epsilon = 1$ the first summand of both formulas zeros. Fig. 2.2.2 shows the squared FCFs for the first 50 vibrational states that were calculated in the framework of this thesis and we will use them later, but first discuss their structure.

The squared FCF's are in all three analyzed cases for the majority of possible transitions almost zero. A range with higher overlap integrals is dominating the process. For $g = 1$ this are the transitions from $\mu = 0$ to $\nu = 0$ (no vibrational energy) or $\nu = 1$. This area forms the angular point of an parabolic shaped high-overlap domain. Like the whole system this parabola is symmetric about exchange of μ and ν. With an increasing vibrational number in the ground state there are in each case of μ two dominating transitions on the mentioned parabola and minor overlaps in between. For $\mu = 20$ these high transitions are to excited states vibrational levels $\nu = 12$ and $\nu = 24$. Outside of the parabola shape the FCF are negligible. The FCF on the parabola are shrinking with increasing the vibrational levels.

In addition to the above mentioned decreasing FCF an enlargement of the PES's energy shift g the shape of the also, but weaker, existing areas of higher overlaps is changed. The parabola shape is preserved but broadened and its angular point is shifted on the $(\mu = \nu)$-diagonal. In the case of $g = 3$ this leads to the disappearance of the $0 \to 0$ transition, but the $3 \to 4$ is majoring as well as the $0 \to 10$ transition.

This analyze of the FCF leads to the conclusion that the arrangement of the PES of the molecules different states is important for the depressing of certain transitions[11].

[11] Note that the inclusion of the FCF in our formulas will depress all transition rates, but some stronger and other weaker.

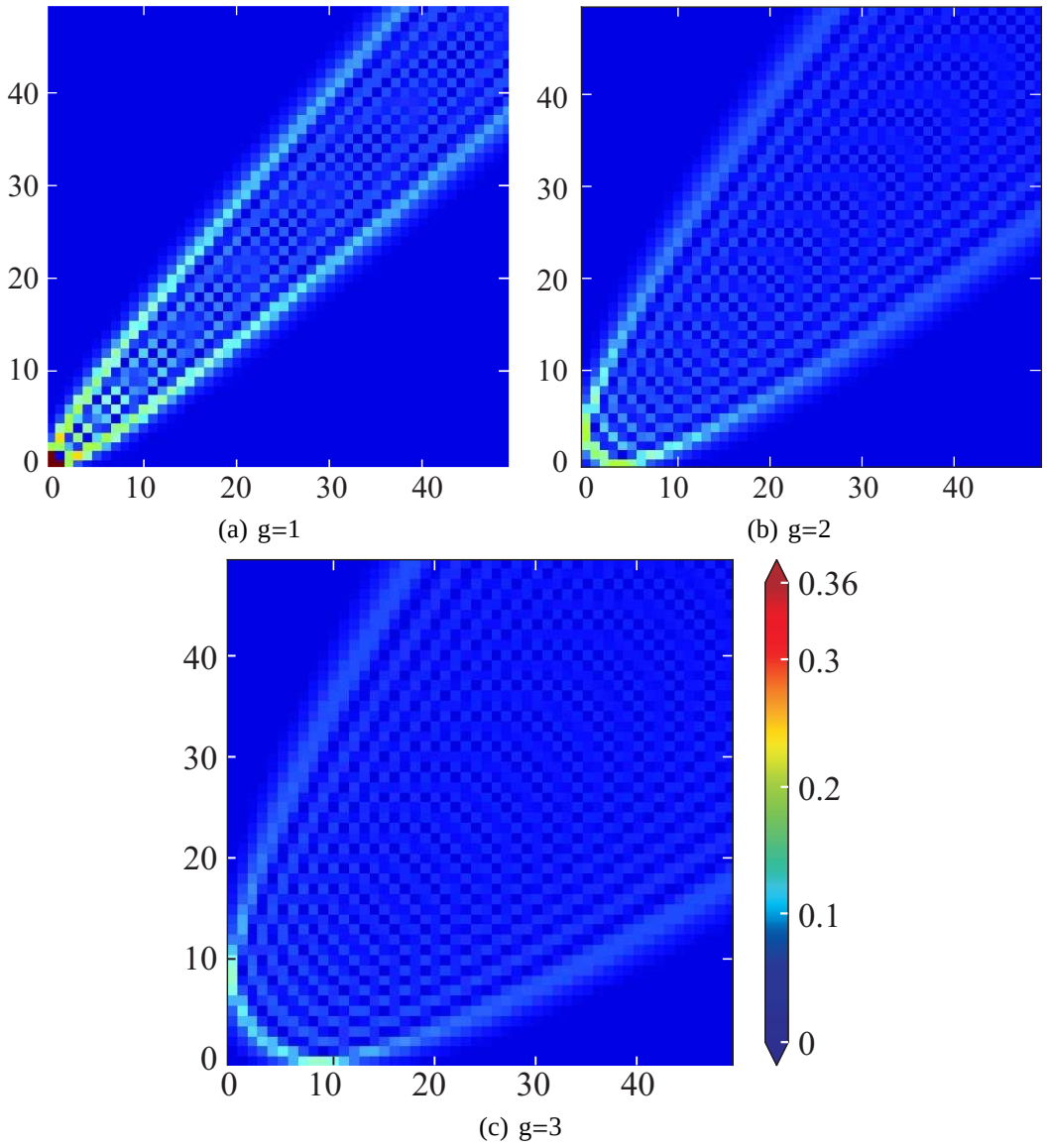

Figure 2.3: Squared FCF with $\epsilon = 1$ for three different choices of g. Note that $g = 1$ refers to charging and exciting of the later discussed molecule, $g = 2$ to only exciting and $g = 3$ to only charging.

2.3 The Hamiltonian of the molecular junction

Above we introduced the Hamiltonian of a single molecule. Since we want to determine the charge transmission through such a molecule attached by nanoelectrodes and with light interaction we have to enlarge the Hamiltonian. The Hamiltonian of the molecular junction is given by

$$H = \underbrace{H_{mol} + H_{field}(t)}_{H_S} + \underbrace{H_{IVR} + H_{mol-lead}}_{H_{S-R}} + \underbrace{H_{sm} + H_{lead}}_{H_R} , \tag{2.26}$$

and the single parts will be discussed below.
The molecular Hamiltonian is given by

$$H_{mol} = \sum_{\alpha} \hbar e_{\alpha} |\psi_{\alpha}\rangle\langle\psi_{\alpha}| , \tag{2.27}$$

whereas $|\psi_{\alpha}\rangle = |\psi_{Na\mu}\rangle$ (Eq. 2.10) are the states and $\hbar e_{\alpha}$ the electron-vibrational spectrum. For further dealing we restrict the discussion to the two charging states neutral ($N = 0$) and singly negatively charged ($N = 1$), the electronic quantum number to ground ($a = g$) and excited state ($a = e$) and the vibrational level to $\mu = 0..n$.
The intramolecular vibrational redistribution (IVR)-Hamiltonian

$$H_{IVR} = \sum_{\alpha,\beta} W_{\alpha\beta} |\psi_{\alpha}\rangle\langle\psi_{\beta}| , \tag{2.28}$$

is written with the introduction of a coupling potential $W(Q, Z)$ between reaction and secondary coordinates (combining all DOF not referring to the reaction coordinate) which we assume to be a bilinear

$$W_{\alpha\beta} = \delta_{Ma,Nb} \sum_{j,\zeta} \hbar k_{j\zeta} \langle\chi_{Na\mu}|Q_i - Q_j^{(Na)}|.\chi_{Na\nu}\rangle Z_{\zeta} \tag{2.29}$$

This enables the relaxation as well as the recurrence of energy and may not change the charging and excitation status, but only the vibrational one. Since it is not necessary we wont specify the Hamiltonian H_{sm} of the secondary coordinates modes.
The Hamiltonian of the leads ($X = L, R$) is formulated with the creation $a^{\dagger}_{X\vec{k}s}$ and annihilation operator $a_{X\vec{k}s}$ for electrons in the spin state s and the band-state $\vec{k}$-vector

$$H_{lead} = \sum_{X,\vec{k},s} \hbar e_{X\vec{k}} a^{\dagger}_{X\vec{k}s} a_{X\vec{k}s}. \tag{2.30}$$

The coupling to the reservoir of the lead electrons allows the change of the charging state

$$\begin{aligned} H_{mol-lead} = \sum_{N,a,b} \sum_{X,\vec{k},s} & V_X(N+1a, Nb, \vec{k}s) a_{X\vec{k}s} |\phi_{N+1a}\rangle\langle\phi_{Nb}| + \\ & + V_X(N-1a, Nb, \vec{k}s) a^{\dagger}_{X\vec{k}s} |\phi_{N-1a}\rangle\langle\phi_{Nb}| , \end{aligned} \tag{2.31}$$

with the transfer integrals $V_X(N \pm 1a, Nb, \vec{k}s)$.
Furthermore we introduce the external fields $\vec{E}(t)$ influence

$$H_{field}(t) = -\vec{E}(t) \sum_{N,a,b} \vec{d}_{Nab} |\phi_{Na\mu}\rangle\langle\phi_{Nb\nu}| , \tag{2.32}$$

with the transition dipole moment $\vec{d}$.
Instead of a strictly monochromatic electromagnetic field a laser pulse of the type

$$\vec{E} = \vec{n}\left(E(t)e^{-i\omega_0 t} + E(t)^* e^{+i\omega_0 t}\right) , \tag{2.33}$$

is used. The center frequency of the pulse spectrum is called *carrier wave frequency* ω_0. We will use two different types of pulse envelopes $E(t)$. Firstly a Gaussian[12] temporal profile

$$E(t) = A \cdot \exp\left(-4\left(\frac{t - t_p}{\tau_p}\right)^2\right), \tag{2.34}$$

with the pulse duration τ_P and the time of pulse maximum r_p is used as the laser pulse. Additionally we will use an switch-on with the shape

$$E(t) = E_0\left(\theta(\tau_s - t)\exp\left(-4\left(\frac{t - \tau_s}{\tau_s}\right)^2\right) + \theta(t - \tau_s)\,,\right) \tag{2.35}$$

with the Heaviside[13] step function $\theta(t - t_0)$. The transition dipole is chosen

$$\vec{n}\vec{d}_{\alpha\beta} = \delta_{M,N}\left(\delta_{a,e}\delta_{b,g}\langle\chi_{Me\mu}|\chi_{Mg\nu}\rangle d_M + \delta_{a,g}\delta_{b,e}\langle\chi_{Mg\mu}|\chi_{Me\nu}\rangle d_M^*\right) , \tag{2.36}$$

so that only transitions with the conservation of the number of electrons and change of the excitation state are allowed. Furthermore we assume that d_M and $E(t)$ are real-valued.

2.4 Charge transmission through a single molecule

The discussion of charge transmission (CT) through single molecules focuses especially on the evocation of a current I by applying a voltage V. Since I is defined as the amount of charge ΔQ moving per time interval Δt we focus on the number of electrons passing from the electrodes to the molecule and backwards. An important attribute is the electrons residence time in the molecule. If it is short in comparison to intramolecular relaxation we name it *direct* transmission otherwise *sequential* CT.
Currently there is no consistent theory to describe this processes. Suitable approaches are e. g. the non-equilibrium Green functions (understanding the CT as a scattering process e.g. [9]), master-equations or the density matrix theory. Here we will concentrate on the latter one for various reasons: Our setting includes vibrational relaxation due to a small molecule lead-coupling. The population of excited electronic states is allowed. And finally the current switching effects by optical excitation is included with emphasis on the temporal evolution.

[12] Carl Friedrich Gauß (1777-1855), Germany
[13] Oliver Heaviside (1850-1925), UK

2.5 Dynamics of open quantum systems

The time dependent Schrödinger equation provides total information about the time evolvement of an isolated quantum system. In general an interaction with other quantum systems has to be taken into account. The dynamics of these *open* quantum systems (S) are way more complicated depending on the environment and particular on its coupling strength. We differentiate between two different kinds of energy flow: *Relaxation* is energy transmission from the system to the surroundings with the possibility of the backward process called *recurrence*. *Dissipation* in contrast means the release of energy from the system to the reservoir and is connected with (in comparison to S) big environments with many degrees of freedom (DOF), since the energy is distributed among themselves. Small microenvironments with a small number of DOF may be calculated in addition to the system S by the Schrödinger equation, whereas a macroscopic reservoir R may be treated by statistical methods.

2.5.1 Density matrix theory

A density matrix describes the statistical state of a quantum system and was introduced by von Neumann[14] in 1927 [10]. Detailed description of the density operator and the density matrix is available in literature (e. g. [8, 11]) and therefore we will give only some major points:
The density operator is given by

$$\hat{W} = w_\nu \sum_\nu |\psi_\nu\rangle\langle\psi_\nu| \tag{2.37}$$

where w_ν are the probabilities to measure the states $|\psi_\nu\rangle$. With the help of a complete orthogonal basis $\{|a\rangle\}$ it can be transformed into

$$\hat{W} = \sum_{a,b} \langle a|\hat{W}|b\rangle |a\rangle\langle b| \tag{2.38}$$

and the coefficients are the *density matrix*

$$\rho_{ab} = \langle a|\hat{W}|b\rangle \tag{2.39}$$

The important equation of motion for the density operator $\hat{W}$ is the *Liouville*[15]*-von Neumann equation*

$$\partial_t \hat{W}(t) = -\frac{i}{\hbar}\left(H\hat{W}(t) - \hat{W}(t)H\right) := [H, W(t)] \tag{2.40}$$

2.5.2 Reduced density matrix

Often we are not interested in the statistical setting $\hat{W}$ of the complete system (S and R) and its time evolution (determined by 2.40), but only in the dynamics of S. This is the

[14] John von Neumann (1903-1957), Hungary-USA
[15] Joseph Liouville (1809-1882), France

keynote of the *reduced density operator*. The starting point for the formation of a reduced density operator is to split the Hamiltonian H into a system part H_S, a reservoir part H_R and the system-reservoir interaction H_{S-R}

$$H = H_S + H_{S-R} + H_R \tag{2.41}$$

with the aim of any basis $|\alpha\rangle$ in the reservoir space we may construct partial trace of the total density operator

$$\hat{\rho}(t) = \sum_{\alpha} \langle\alpha|\hat{W}(t)|\alpha\rangle = \mathrm{tr_R}\left(\hat{W}(t)\right) \tag{2.42}$$

which is named the reduced density operator and includes only the dynamics of S with inclusion of the interaction between R and S in a limited order.

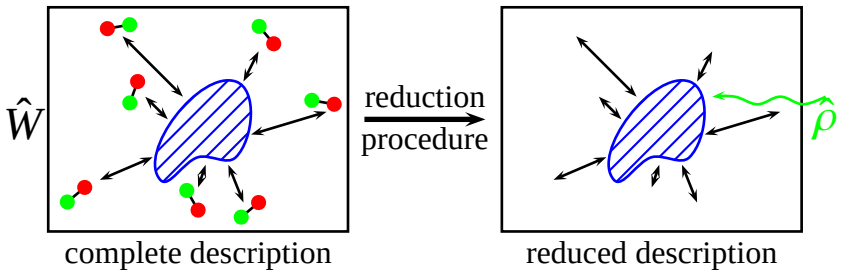

Figure 2.4: The total statistical description by $\hat{W}$ is replaced by the reduced statistical operator $\hat{\rho}$ which includes the system dynamics and the interaction between the system and the reservoir. After [6].

In [12] a setting similar to ours was investigated. But instead of taking into account all elements of the density matrix $\rho_{\alpha\beta}$ developed in [3] the off-diagonal elements were neglected and so reduced to a rate equation formulation. We want to include the off-diagonal elements in our calculations of the time-evolution, while taking in mind that $\rho_{\alpha\beta} = \rho^*_{\beta\alpha}$. Note that the off-diagonal elements can be understood as coherences of different states and will not be analyzed themself, since we are only interested in the electron-vibrational states populations characterized by the diagonal elements $\rho_{\alpha\alpha}$.

2.6 The reduced density operators equation of motion

Finally we obtain the equation of motion for the reduced density matrix of the form

$$\partial_t \rho_{\alpha\beta}(t) = i e_{\alpha\beta}\rho_{\alpha\beta}(t) + (\partial_t \rho_{\alpha\beta})_{dissi}\,, \tag{2.43}$$

with the transition frequencies $e_{\alpha\beta} = e_\alpha - e_\beta$. In our case with included external field driven dynamics we receive

$$\begin{aligned}\partial_t \rho_{\alpha\beta}(t) = &- i e_{\alpha\beta}\rho_{\alpha\beta}(t) + \frac{i}{\hbar}\vec{E}(t)\sum_{\gamma}\left(\vec{d}_{\alpha\gamma}\rho_{\gamma\beta}(t) - \vec{d}_{\gamma\beta}\rho_{\alpha\gamma}(t)\right) + \\ &\underbrace{+\,\delta_{\alpha,\beta}\sum_{\gamma}\left(k_{\gamma\to\alpha}\rho_{\gamma\gamma}(t) - k_{\alpha\to\gamma}\rho_{\alpha\alpha}(t)\right) - (1-\delta_{\alpha,\beta})r_{\alpha\beta}\rho_{\alpha\beta}(t)}_{(\partial_t\rho_{\alpha\beta})_{dissi}}\,,\end{aligned} \tag{2.44}$$

where we have introduced different rates we will examine now:
The following dephasing rates

$$r_{\alpha\beta} = \frac{1}{2}\sum_{\gamma}\left(k_{\alpha\to\gamma} + k_{\beta\to\gamma}\right) + r^{pd}_{\alpha\beta}\,, \tag{2.45}$$

which enables the decay of the off-diagonal elements of the density matrix and may be amplified by the pure dephasing contribution $r^{pd}_{\alpha\beta}$. Transition between different states are enabled by interaction with an extern reservoir given by the Hamiltonian H_{S-R}. Here we treat with two different types, molecule-lead coupling and IVR as coupling to the secondary coordinates too:

$$k_{\alpha\to\beta} = k^{mol-lead}_{\alpha\to\beta} + k^{IVR}_{\alpha\to\beta} \tag{2.46}$$

The charging is given by

$$k^{mol-lead}_{0a\mu\to 1b\nu} = 2|\langle\chi_{0a\mu}|\chi_{1b\nu}\rangle|^2 \sum_{X}\Gamma_{Xab}\, f_F\left(\hbar e_{1b\nu,0a\mu} - \mu_X\right)\,, \tag{2.47}$$

and discharging by

$$k^{mol-lead}_{1b\nu\to 0a\mu} = 2|\langle\chi_{1b\nu}|\chi_{0a\mu}\rangle|^2 \sum_{X}\Gamma_{Xab}\left(1 - f_F\left(\hbar e_{1b\nu,0a\mu} - \mu_X\right)\right). \tag{2.48}$$

Note the introduction of the factor 2 for the spin-up and spin-down states of the electrons since we foregoing neglected the spin states. The Fermi[16]-distribution f_F handles the energy of the leads electrons at a temperature T and an chemical potential of μ. To simplify matters we introduce a molecule-lead coupling Γ_{Xab} which contains the transfer integrals $V_X(N \pm 1a, Nb, \vec{ks})$. In our discussion Γ wont be depending on the charging states or the lead and will be fixed.
Finally we specify the rate of IVR in the case of the bilinear-coupling model with a single reaction coordinate Q to

$$k^{IVR}_{Ma,\mu\to\nu} = \frac{2\pi}{\hbar} J_{Ma}(\omega_{vib})\left(\delta_{\nu,\mu-1}\mu(1 + n(\omega_{vib})) + \delta_{\nu,\mu+1}(\mu+1)n(\omega_{vib})\right)\,, \tag{2.49}$$

where we fix the spectral density $J_{Ma}(\omega_{vib})$. $n(\omega_{vib})$ denotes the Bose[17]-Einstein[18]-distribution.

2.6.1 Coupling to a laser pulse

In order to remove the fields fast oscillations from the density matrix equations (2.44) we have to reformulate it. The introduction of a reduced notation only including the electronic quantum numbers (e,g) and furthermore

$$\sigma_{eg}(t) = \exp(+i\omega_0 t)\rho_{eg}(t)\,, \tag{2.50}$$

[16] Enrico Fermi (1901-1954), Italy-USA
[17] Satyendranath Bose (1894-1974), India
[18] Albert Einstein (1879-1955), Germany-USA

leads to a transformed density-matrix σ_{ab}. In the next step we apply the *Rotating Wave Approximation*. This enables to neglect of the fast oscillating filed terms and we finally arrive a set of four equations:

$$\partial_t \sigma_{gg} = \frac{i}{\hbar} E(t) \left(d_{ge}\sigma_{eg}(t) - d_{eg}\sigma_{ge}(t) \right) + (\partial_t \sigma_{gg})_{dissi} \tag{2.51}$$

$$\partial_t \sigma_{ee} = \frac{i}{\hbar} E(t) \left(d_{eg}\sigma_{ge}(t) - d_{ge}\sigma_{eg}(t) \right) + (\partial_t \sigma_{ee})_{dissi} \tag{2.52}$$

$$\partial_t \sigma_{eg} = -i(e_{eg} - \omega_\gamma)\sigma_{eg} + \frac{i}{\hbar} E(t) d_{eg}(\sigma_{gg} - \sigma_{ee}) + (\partial_t \sigma_{eg})_{dissi} \tag{2.53}$$

$$\partial_t \sigma_{ge} = -i(e_{ge} + \omega_\gamma)\sigma_{eg} + \frac{i}{\hbar} E(t) d_{ge}(\sigma_{ee} - \sigma_{gg}) + (\partial_t \sigma_{ge})_{dissi} \tag{2.54}$$

Note that the diagonal elements are the same as in 2.44 and this allows us to analyze them without retransformation.

2.6.2 Current formula

The total current hat each of the leads (X=L,R) can be calculated with

$$I_X(t) = I_{X,0\to1}(t) + I_{X,1\to}(t). \tag{2.55}$$

The current due to charging and discharging is given by

$$I_{X,0\to1}(t) \approx 2|e| \sum_{a\mu,b\nu} \Gamma |\langle \chi_{0a\mu} | \chi_{1b\nu} \rangle|^2 f_F \left(\hbar e_{1b\nu,0a\mu} - \mu_X \right) \sigma_{0a\mu,0b\nu}(t) \,, \tag{2.56}$$

and the discharge by

$$I_{X,1\to0}(t) \approx -2|e| \sum_{a\mu,b\nu} \Gamma |\langle \chi_{0a\mu} | \chi_{1b\nu} \rangle|^2 \left(1 - f_F \left(\hbar e_{1b\nu,0a\mu} - \mu_X \right) \right) \sigma_{0a\mu,0b\nu}(t). \tag{2.57}$$

3. Numerical calculations

3.1 Choice of parameters

The simulations do not refer to a certain molecule with locked characteristics. Rather we will discuss a variation of the parameters. We assume that the molecule is located in the middle between the both nanoelectrodes. Then the chemical potentials of the both electrodes can be calculated within the model of a *symmetrically applied voltage* at the left (L) and right (R) lead

$$\mu_L = \mu_0 + |e|\frac{V}{2} , \tag{3.1}$$

$$\mu_R = \mu_0 - |e|\frac{V}{2} , \tag{3.2}$$

whereas μ_0 is the chemical potential of the leads in absence of an applied voltage V and will be set zero below.
Furthermore we define the so called charging energy

$$\Delta E_{10} = E_{1a} - E_{0a} - \mu_0 , \tag{3.3}$$

which will be identical for excited (e) and ground state (g).
For further considerations it is advisable to replace the molecule-lead coupling by one single constant Γ. Since our approach is suited for hopping charge transmission we will reduce the discussion to weak and intermediate strength of the coupling. The influence of the number of calculated vibrational n levels will be discussed and consequently fixed to 20. Our choice of k_BT refers to a temperature of about 35 K.
The influence of the external field is firstly characterized by the product of the fields amplitude and the molecules transition dipole moment the so called *Rabi*[1]*-energy*

$$E_R = \vec{d}\vec{E}. \tag{3.4}$$

The Rabi-energy of the external fields steady state dE_0 is chosen to 1 meV which refers to an electric field strange of $10^7 \frac{\mathrm{V}}{\mathrm{m}}$ and a transition dipole moment of about 5 D[2]. We will reduce our discussion to short-time laser pulses with widths of 0.5 and 5 ps.
The influence of IVR is determined by the value J and is varied between 0 (no IVR) and 1 meV, which results in a first excited vibrational states lifetime ($\frac{\hbar}{2\pi J}$) of about 0.1 ps. We

[1] Isidor Isaac Rabi (1898-1988), USA
[2] 1 Debye = $3.33564 \cdot 10^{-30}$ Cm, after Peter Debye (1884-1966), Netherlands-USA

Parameter	Standard value	Variation	Unit
n	20	2…30	–
U	0.75	0…2	V
$\Gamma\hbar$	1	0.1	meV
J	1	0; 0.1	meV
τ_s	0.5	5	ps
$\hbar\omega_{vib}$	62.5	–	meV
ΔE_{10}	0.5	–	eV
E_C	2	–	eV
$E_R = Ad$	1	–	meV
$\hbar\omega_0$	2.25	–	eV
μ	0	–	eV
k_BT	3	–	meV
Q_{0g}	0	–	–
Q_{0e}	2	–	–
Q_{1g}	3	–	–
Q_{1e}	1	–	–

Table 3.1: Sets of parameters. If not mentioned otherwise the *Standard value* is used.

reduce the discussion to one single reaction coordinate Q with the PES

$$U_{Na}(Q) = U_{Na}(Q)^{(0)} + \frac{\hbar\omega_{vib}}{4} \cdot \left(Q - Q^{(Na)}\right)^2 \ , \tag{3.5}$$

whereas the vibrational frequency ω_{vib} is independent on the electronic state. The arrangement of the PES with the equilibrium values $Q_{(Na)}$ and the energy at these configurations $U_{Na}(Q)^{(0)}$ is shown in Fig. 3.1.
In the initial condidition for our calculations we take the molecule to be completely relaxed and in the noncharged ground state, e.g. the probibility to be in state $|\psi_{0g0}\rangle$ is 1 and for all other states it is 0.

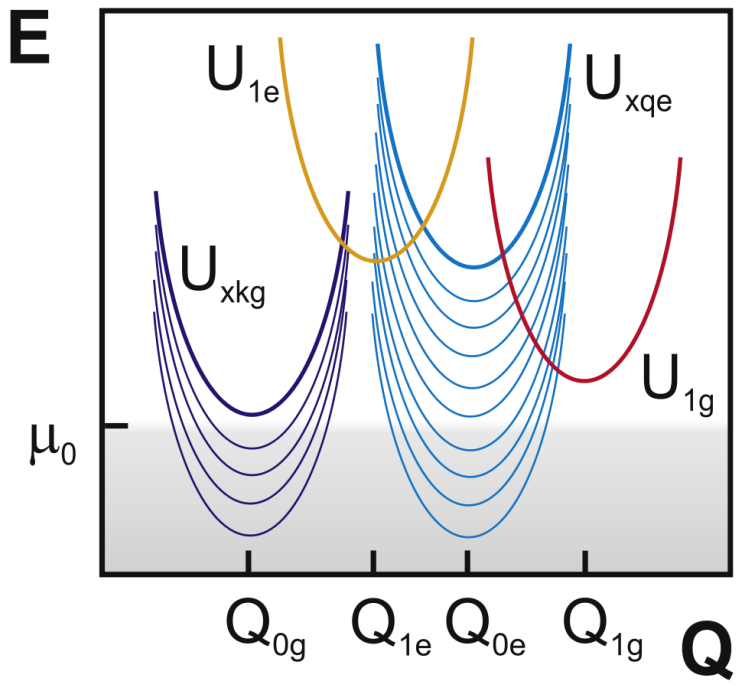

Figure 3.1: Arrangement of PES [4]; energies below the chemical potential μ_0 are shown in a grey shade. The neutral states PES form a continuum since they combine the energy with the leads electrons energy. The dimensionless shift of the PES Q influences the FCF and these the transition rates. Note that while the relative arrangement of the PES is equal to the work done in [4] the absolute values used in our calculations are halved in order to receive stronger currents.

3.2 Programm

The flowchart of the program designed to solve the reduced density matrix equations of motion is pictured below. The input parameters (red) are configured in Tab. 3.1 and may be changed for future considerations. The calculations are undertaken one after another from the top (first: FCF $\langle\Psi_{aM}|\Psi_{bN}\rangle$) downwards (last: current I). The solving of the ordinary differential equation (ODE) takes at this the most computational time. The program was written in the programming language Python, using various libraries. The resulting complex-valued ODE was solved with the ZVODE method based on the VODE-algorithm published by Brown et. al. in 1989 [13].

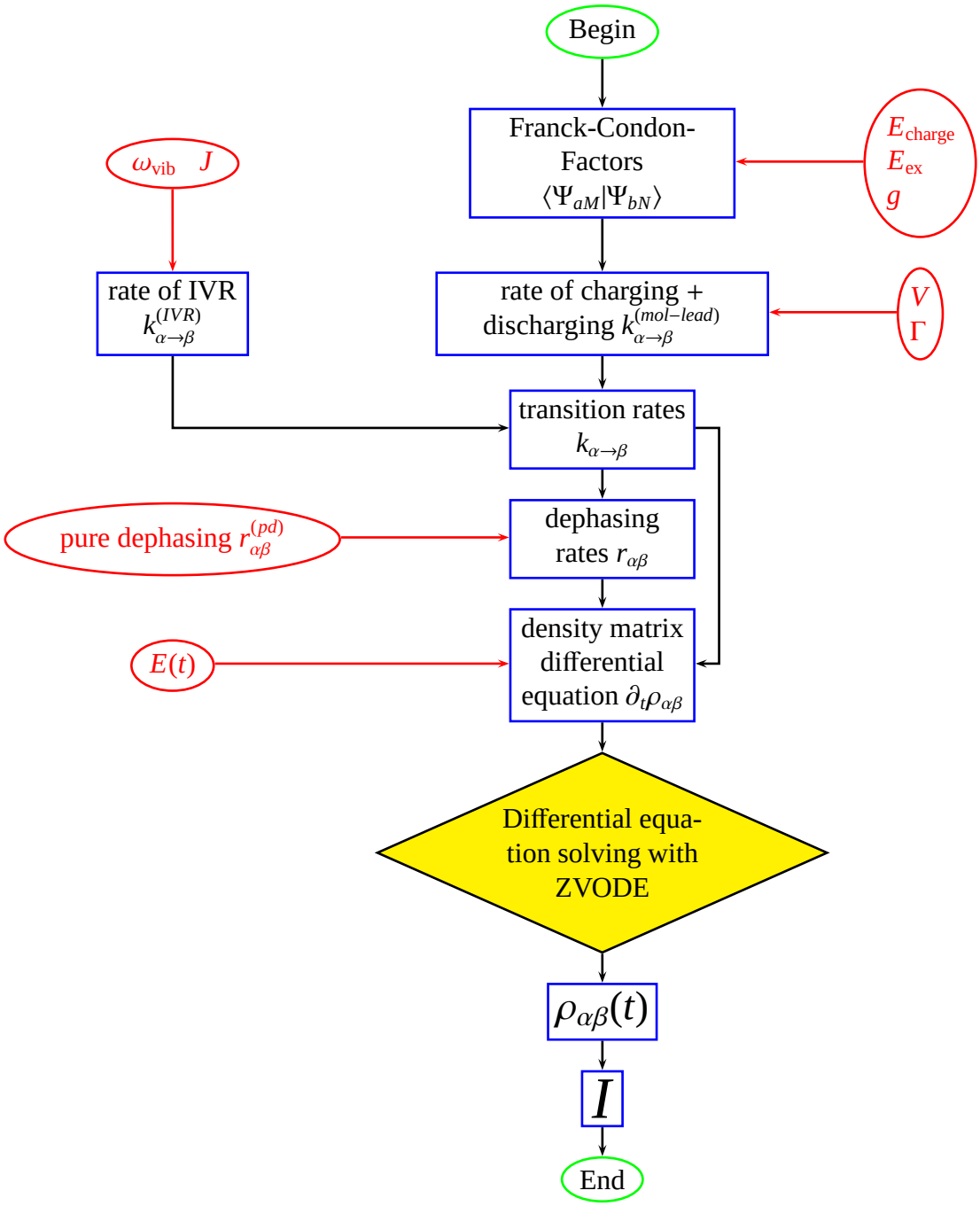

4. Results

4.1 Inclusion of vibrational levels

An important issue in the numerical calculation of transient currents is the restriction to a finite number of vibrational levels. In reality the number of populated vibrational levels is not limited but the numerical calculation allows only a reduced inclusion. Fortunately the form of the FCF (cf. 2.2.2) as well as the restriction to a finite applied voltage enables this: Former research (e.g. [3]) has shown that the current flow may be understood as charging and discharging processes between the molecule and both electrodes. The effectiveness of them is critically determined by the FCF. We have shown that for our setting the FCF are decreasing with higher vibrational levels, hence we assume that the neglect of charging and discharging processes via high vibrational levels has only minor influence on the final results.
To test this we calculated the charging process at an applied voltage of 1.5 V for 6 different choices of n (5,10,15,20,25,30). The calculation shows that the time-resolved formation of the stationary current is generally dependent on n, but is subject to saturation. This results in nearly unchanged stationary results Fig. 4.2(b) for $n > 20$, where we took the stationary current I_{stat} and the time it is reached t_{stat} as the characteristic numbers. Furthermore the charging processes over time Fig. 4.2(a) is only minor affected by increasing the number of vibrational levels over 20. This behavior will be discussed below, for now only taking the information, that we may reduce our calculations to 20 vibrational levels.

4.2 Steady-state current: IV-characteristics

4.2.1 Without optical excitation

For understanding the photoswitching of currents it is firstly advisable to discuss the formation of steady-state currents at absence of photoexcitation. The stationary situation is given with $I_L = -I_R$, i.e. the charge is flowing in same amount from the left electrode on the molecule and from the molecule continuing to the right electrode[1], no net charge is placed on the molecule. Of main interest in the time-independent situation is the shape of IV-characteristics Fig. 4.4. The calculation was done for 3 different choices of IVR-strength belonging to vibrational relaxation times of $\tau_{IVR} = 0.1$ ps, 0.5 ps and disabled IVR. Since the charging energy is chosen to 0.5 eV from 1 V on a current may flow. The step-like form of the IV-characteristics is remarkable and will be discussed below:

[1] While this picture is correct nevertheless, we have especially in mind that the potential at the left electrode is higher than at the right electrode due to the applied voltage.

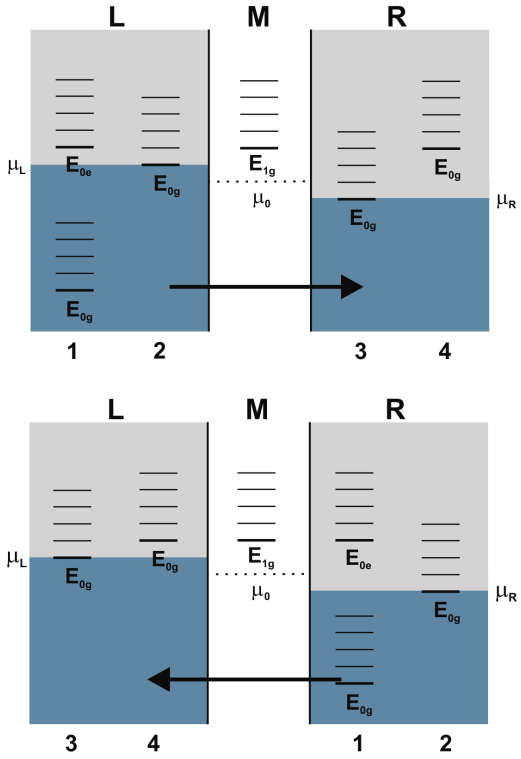

Figure 4.1: Energetics of sequential charge transmission at a presence of small applied voltage. Light-grey: Unpopulated lead electron levels above the Fermi sea, Blue: Populated lead electron levels inside the Fermi sea. Upper panel shows the left → right charge transmission and the lower the backward process. 1 shows initial energetic states for photoinduced CT and 2 at absence of optical excitation. 3 and 4 are possible final state energy levels. Charge transmission can be pictured as a horizontal movement in this scheme. [4]

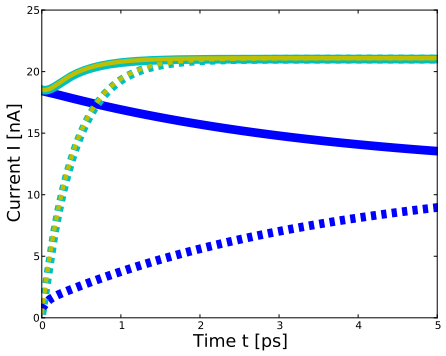

(a) Current over time for n =5 (blue),20 (cyan),30 (yellow). Note that the last ones have nearly the same shape. Dotted line $-I_L$, solid line I_R.

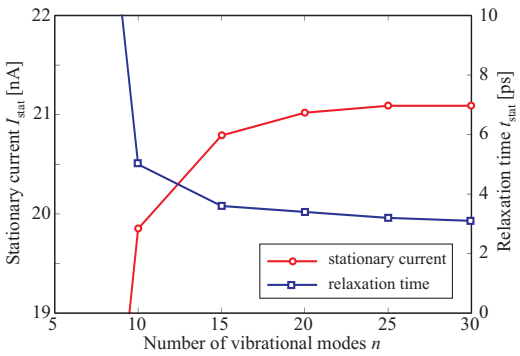

(b) Stationary current

Figure 4.2: Influence of number of calculated vibrational levels on (a) the shape of the current over time and (b) the stationary current I_{stat} as well as the relaxational time in which it is reached t_{stat} with an applied voltage of $V = 1.5\,\mathrm{V}$

The charging process may be understood as the molecules transfer from an uncharged quantum state $|\psi_{0a\mu}\rangle$ to a charged one $|\psi_{1b\nu}\rangle$. This is allowed if there are electrons in the leads whose energy is higher than the charging energy of the molecule. We will account the leads electrons energy with E_{el}. Thus the relation $\hbar e_{0a\mu} + E_{el} = \hbar e_{1b\nu}$ has to be fulfilled to enable the transition including charging. Furthermore the state $|\psi_{0a\mu}\rangle$ has to be populated. Our choice of a low temperature let the population stay mainly in the vibrational ground-state. Consequently the transition from $|\psi_{0a0}\rangle$ to different excited states $|\psi_{1bv}\rangle$ is dominating transitions from other electric states. If the charging energy is almost reached only the transition to the vibrational-ground state of the charged molecule $|\psi_{1g0}\rangle$ is allowed (as indicated in the arrangement 2 of the upper panel in 4.1). With further increasing of the applied voltage also the charging through other transitions e.g to the higher lying $|\psi_{1a1}\rangle$ becomes possible. This leads to the step-like IV-characteristics whereat the edges are rounded by the influence of the Fermi-distributed lead-electrons energy. Every step can be pictured as a new transmission channel for chargeflow onto the molecule and therefore through the molecule since discharge to the right electrode is not limited in this range: The discharging of the molecule to the right electrode is energetically allowed for various final states $|\psi_{0a\mu}\rangle$ and a population of the vibrational excited states in both the charged and the neutral molecule becomes possible (right side of upper panel of4.1)). It is important to underline that also the backwards transition as a charging of the molecule from the right electrode and discharge to the left electrode is possible for high vibrational states (lower panel of Fig. (4.1)). Since the vibrational ground states are mainly populated at low temperatures the contrary current is quite smaller then the left-right current and we receive a net current above zero. Furthermore it is accountable that the steps in the IV-characteristics are of different height. This is generated by the Franck-Condon-factors (2.2.2). With our choice of parameters the charging-process is connected with a dimensionless PES-shift of 3. In this configuration e.g. the transmission from vibrational ground-state of the uncharged molecules PES to the ground-state of the charged molecules PES is suppressed and leads to a quite small first step.
Past work [4] using rate equations showed the step formation of the stationary IV characteristics by underlining the importance of the FCF too. The difference in the absolute seize of the currents (Wang and May calculated a current of about 60 nA at an applied voltage of 2 V) are caused by our reduced distance in the reaction coordinate Q. This leads to enlarged FCF and hence to an amplified charge flow.

4.2.2 With optical excitation

Furthermore we will discuss the influence of an optical excitation to the generated steady-state current. This is calculated with a switching-on laser-pulse (2.35) finally resulting in a constant Rabi-energy of 1 meV. The excitation of the molecule allows transitions of the form $\hbar e_{0e\mu} + E_{el} = \hbar e_{1ev}$ and even at an applied voltage below the in foregoing case needed of 1 V charge injection from the left electrode can be observed (1 in upper panel of 4.1). In contrast to the case without optical excitation a wide range of final vibrational states $|\psi_{1gv}\rangle$ is energetic reachable. While the charging is possible from both electrodes with the same strength the discharge process is important for the net current. The discharge to the energetic higher left electrode is taking place, but the discharge to the right electrode has more transitions available. This behavior shows the importance of vibrational levels and confirms the own result [2] that such optical switching behavior is not realizable for a sys-

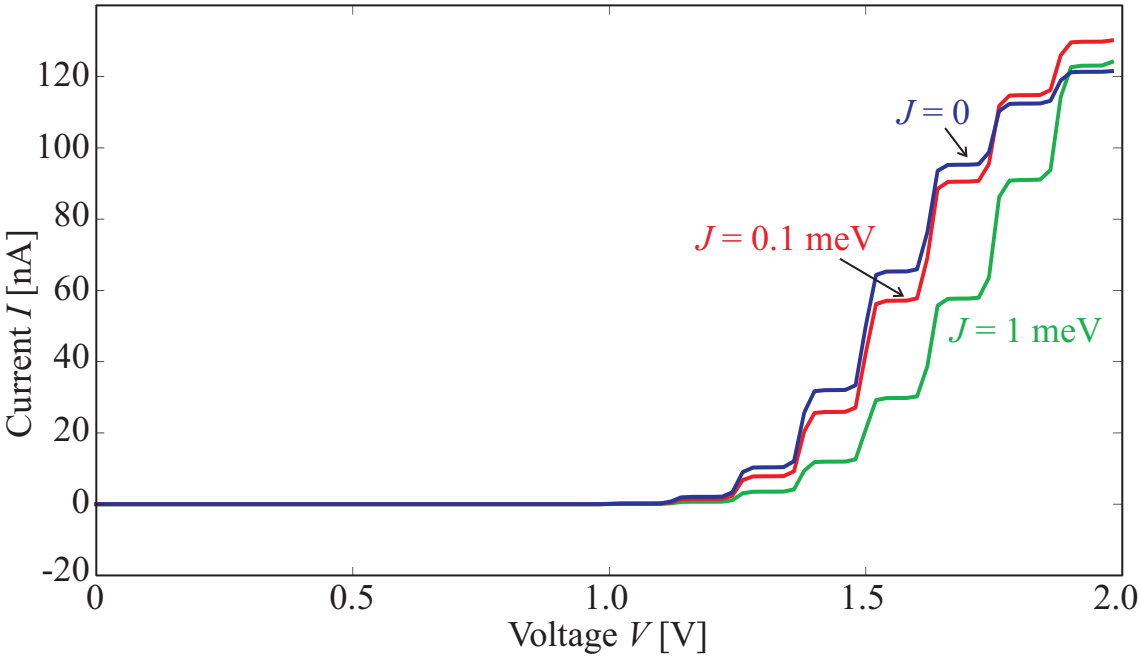

Figure 4.3: IV-characteristics at absence of optical excitation for 3 choices of IVR-strength: Blue line $J = 0$, Green line $J = 1$ meV, Red line $J = 0.1$ meV

tem without vibrational levels[2]. A variation of IVR-strength underlines the importance of vibrational levels. In the case of infinite IVR lifetimes the switching behavior is stronger than for activated IVR. Since the molecule is located in the lower vibrational states more often under the influence of IVR the difference in discharging channels for the both electrodes is reduced. The extreme limit would be an IVR lifetime much smaller than the electrons residence time in the molecule. This accumulates the population exclusively in the vibrational ground state, no net current is obtained and therefor switching becomes impossible (not shown in IV-characteristics).

4.3 Population of the electron-vibrational states over time

The forth going analysis has underlined the importance of the population of vibrational levels for the processes leading to a net current under influence of an optical field, when otherwise no current appears. To visualize the population of all electron vibrational states over time we created matrix plots (Fig. 4.5 - 4.8) with a logarithmic color bar. White means no population and dark red stands for high population. Each of them is compound of 4 subplots (one for each electric state) next to each other. The subplot itself shows the population of the 20 vibrational levels and their time development on the ordinate in discrete time steps of 1 ps. In every plot the voltage is fixed at $U = 0.75$ V. We should take in mind that the initial state was given by only populating the $|\psi_{0g0}\rangle$ state with a chance of 1.

The first arrangement is without optical excitation. The first fact we immediately see is that both excited states stay unpopulated over the whole time. Both electrical ground states are populated, including all vibrational levels, at which the energetic deeper laying

[2] A weak switching behavior was only detectable for asymmetric molecule-lead couplings.

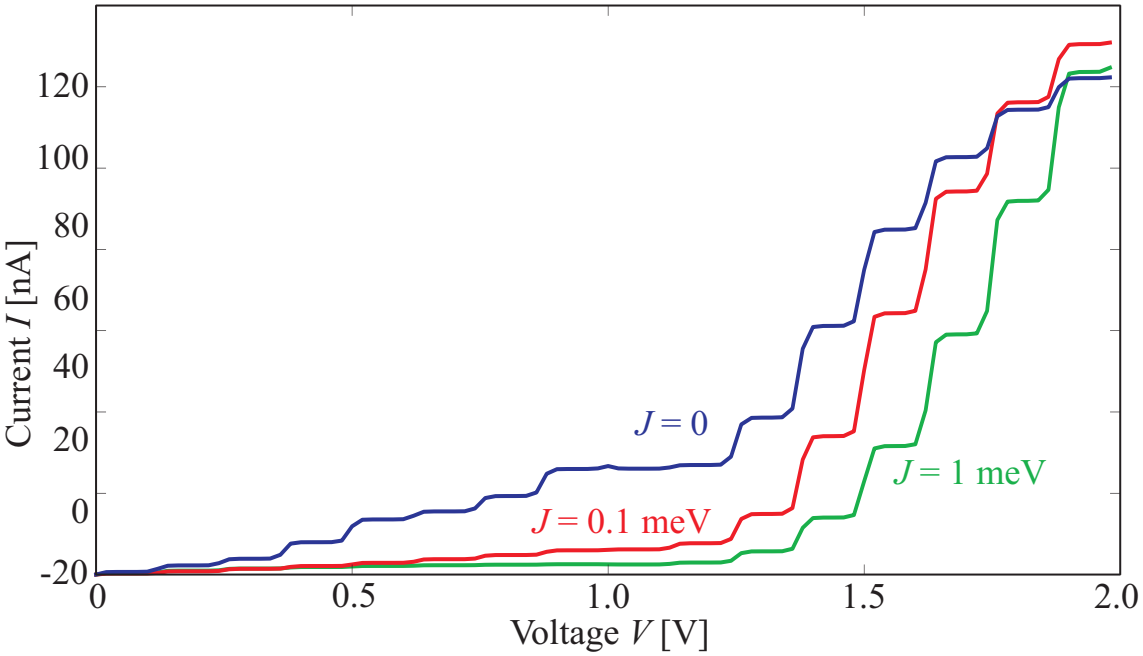

Figure 4.4: IV-characteristics with optical excitation for 3 choices of IVR-strength: Blue line $J = 0$, Green line $J = 1$ meV, Red line $J = 0.1$ meV

states are more populated. A look at the first time-step shows that it takes less then 2 ps to reach a equilibrium situation, since afterwards nearly no change is detectable. Taking Fig. 4.1 and the charging mechanism explained previous we may interpret the population of the first charged state as charging from both leads from $|\psi_{0g0}\rangle$ to $|\psi_{0g\mu}\rangle$ due to the small amount of lead electrons above the Fermi sea with enough energy to get over the necessary charging energy of 0.5 eV. In the first time step we see that firstly the charged state is populated and afterwards an equilibrium is reached. This process involves discharging to any uncharged ground state (following in population of all states $|\psi_{0g\mu}\rangle$), but the population is concentrated in the energetic deeper vibrational levels due to IVR.
We now want to analyze the influence of a 5 ps long Gaussian laser pulse. Firstly we see that all electron-vibrational states are populated when the light is active. The optical excitation enables immediately and with raising intensity the transition from $|\psi_{0g0}\rangle$ to $|\psi_{0e\mu}\rangle$. The population of the excited state again gives the energetic condition for population of the charged ground state via molecule-lead electron transfer. As mentioned before that this process is the same on both electrodes. The charged ground state itself may be excited by the external field and so the population of the $|\psi_{1e\mu}\rangle$ is enabled. We also see that at the time of maximal field strength nearly all vibrational levels of the $|\psi_{0g\mu}\rangle$ are strongly occupied. This underlines the fact that discharge and deexcitation are not only ending in the vibrational ground state, but rather populate all of them. After the decay of the optical field the population is slowly returning to the uncharged vibrational ground state. This self stabilization behavior was already detected in [4] and can be understood as follows: We choose the symmetrically applied voltage of 0.75 so that it makes charge injection only for the minority of the leads electrons possible. They have to reach at least an energy of 0.5 eV and this lies 0.125 eV above the fermi-sea . After (in fact also within) the Gaussian laser pulse the population is distributed over all electron-vibrational levels. Now transitions from energetic lower levels under usage of vibrational energy as well as

the lead electrons energy are possible. Since $\hbar\omega_{vib} = 62.5\,\text{meV}$ is the energy step of a single vibrational level at least $\Delta\mu = 2$ is necessary to enable the $|\psi 0g\mu\rangle \rightarrow |\psi 1g(\mu - \Delta\mu)\rangle$ transition.
Furthermore we want to inspect the same situation but with disabled IVR. We immediately see that the process in the beginning is slowed down: Only a fraction of the population is leaving the $|\psi_{0g0}\rangle$ state and entering the other states. An exception is the transition to the $|\psi_{0e0}\rangle$ state: Due to the FCF this transition is the with the highest rate and therefore not slowed down by deactivating IVR. The $|\psi_{0e0}\rangle$ itself enables the population of the $|\psi_{1g\mu}\rangle$ states but charging through this one channel is much slower as with the more as in the foregoing case which underlines the importance of IVR: IVR spreads population from the vibrational ground level to higher ones and therefore activates more charging channels. After the laser pulse the influence of IVR is not wished. As we see the population stays longer in the higher energetic states. Especially the $|\psi_{1g\mu}\rangle$ state looses population only slowly to the $|\psi_{0g\mu}\rangle$ states via electron transfer between leads and molecule. With this process the higher vibrational levels are left and the population is concentrated again in the $|\psi_{0g\mu}\rangle$ states. The comparison between Fig. 4.7 and Fig. 4.6 shows that this process is much slower without IVR since in this case more transition channels are usable.
Al last we ant to determine the influence of the molecule-lead coupling Γ. Its reduction leads to a longer residence time of the electron in the molecule. All charging-discharging processes take longer and therefore more population is accumulating in the uncharged excited state since the population may leave the state to the $|\psi_{1g\mu}\rangle$ slower. After the laser pulse is faded the above mentioned processes of accumulating in the $|\psi_{0g\mu}\rangle$ states are observable but also much slower since the interaction with the lead electrons is needed to change the electronical state.

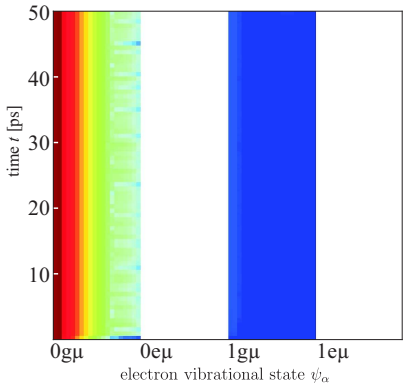

Figure 4.5: Population of states (including vibrational levels) over time in case of limited charging ($U = 0.75\,\mathrm{V}$). Charged state is slowly populated due to small number of lead electrons with energy $> \Delta E_{10}$. Without optical excitation. Excited states are unpopulated.

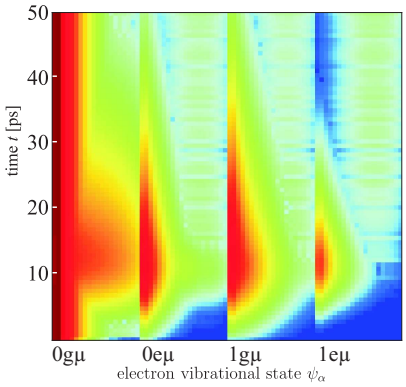

Figure 4.6: Population of states (including vibrational levels) over time in case of limited charging ($U = 0.75\,\mathrm{V}$) with optical excitation by a 5 ps long Gaussian laser pulse with maximum at 10 ps. Due to excitation all states are populated.

4.4 Switching: Optical excitation with Gaussian laser pulses

In the following we will analyze the time-resolved behavior of the current flow through a single molecule excited with an optical field. At absence of steady-state situations it becomes important to distinguish the current $I_L(t)$ passing from the left lead into the molecule and the negative current $-I_R(t)$ passing from the right electrode into the molecule. We want to introduce the temporal net charging of the molecule

$$\partial_t Q_{mol}(t) = -\left(I_L(t) + I_R(t)\right) \tag{4.1}$$

For $I_L(t) > -I_R(t)$ the molecule is charged and otherwise charge is leaving the molecule. Foregoing we have shown that in a case of an applied voltage of $V_{appl} = 0.75\,\mathrm{V}$ a current appeared only under optical excitation. Therefore the construction of an an optical switch seems possible. Firstly we want to discuss the behavior of a short laser pulse with a width of 0.5 ps and a field maximum at 3 ps (4.5). Is is notable that $-I_R$ becomes negative until

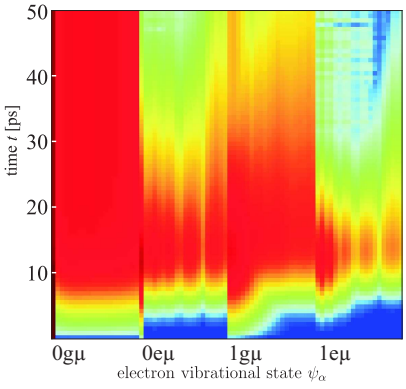

Figure 4.7: Population of states (including vibrational levels) over time in case of limited charging ($U = 0.75\,\mathrm{V}$) with optical excitation by a 5 ps long Gaussian laser pulse with maximum at 10 ps. IVR is surpressed ($J = 0 \rightarrow \tau_{IVR} = \infty$).

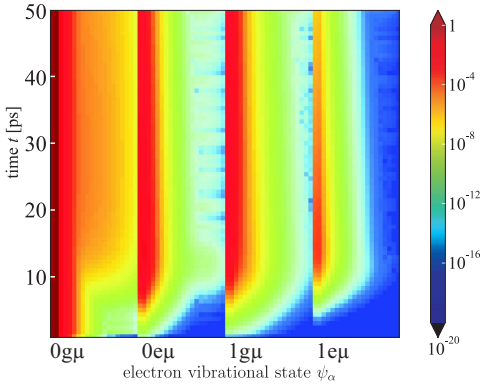

Figure 4.8: Population of states (including vibrational levels) over time in case of limited charging ($U = 0.75\,\mathrm{V}$) with optical excitation by a 5 ps long Gaussian laser pulse with maximum at 10 ps. Molecule-lead coupling is ten times smaller ($\hbar\Gamma = 0.1\,\mathrm{meV}$)

a time of about 2.5 ps. This means that charge is flowing from both electrodes inside the molecule, resulting in no net current through the molecule. This behavior is not dependent on the strength of IVR. Afterwards a net current can be calculated since charge flows from the left electrode into the molecule and furthermore charge from the molecule to the right electrode, since $I_L > -I_R$ the molecule is charged. Shortly after the laser pulse maximum the currents at both leads are decreasing, whereat the left leads reaction is faster and declines about one ps earlier. Here the influence of IVR is significant: While at slow IVR and absence of IVR $-I_R$ is further increasing and reaches a maximum above the one of I_L in the case of $J = 1\,\mathrm{meV}$ both currents have nearly the same maximum height. Afterwards $-I_R > I_L$ and thus the molecule is discharged. This process is also strongly coupled to the influence of IVR, since at absence of IVR the molecule is only slowly discharging and stays charged way longer then the 50 ps we have drawn. We explained this behavior already in the foregoing section, but want now underline that this self-stabilized behavior not only let the molecule stay in the energetic higher states for a time much longer than the puls durance, but also leads to a usable net current. In order to understand this we have to take a look at Fig. 4.1 at the situation without optical excitation. Firstly the charging from the left electrode is enabled since the higher vibrational levels are still occupied. This discharge is again no problem and is possible for a large range of transitions. The charging from the right electrode may possible due to the excited vibrational states but the applied voltage leads to a shift that prefer the transition from the left electrode on the molecule. Consequently a net current is observable.

In Fig. 4.4 the current over time for a Gauss shaped laser pulse of 5 ps length and the field maximum at 10 ps is shown. The shape of the curves is quite similar to the situation with the shorter pulse, especially the strong self-stabilization process can be detected at absence of IVR. The main difference to the foregoing discussion is the maximal current and the amplified difference between the 3 curves. Obviously a longer laser pulse with the same maximal field strength carries more energy in the molecule, enables more excitation and therefore a larger photoinduced current. In our case the maximal photocurrent is twice the amplitude of the small laser pulse.

Former calculations with rate equations [12] on the time-resolved current through a single molecule while exciting with a Gauss shaped laser pulse came to similar but also slightly different results. The formation of photo induced current is reproduced with emphasis on the self-stabilization mechanism that is amplified by reducing the IVR strength. As already mentioned at the part of the stationary currents the occurring currents are twice the height in our calculation due to closer PES.

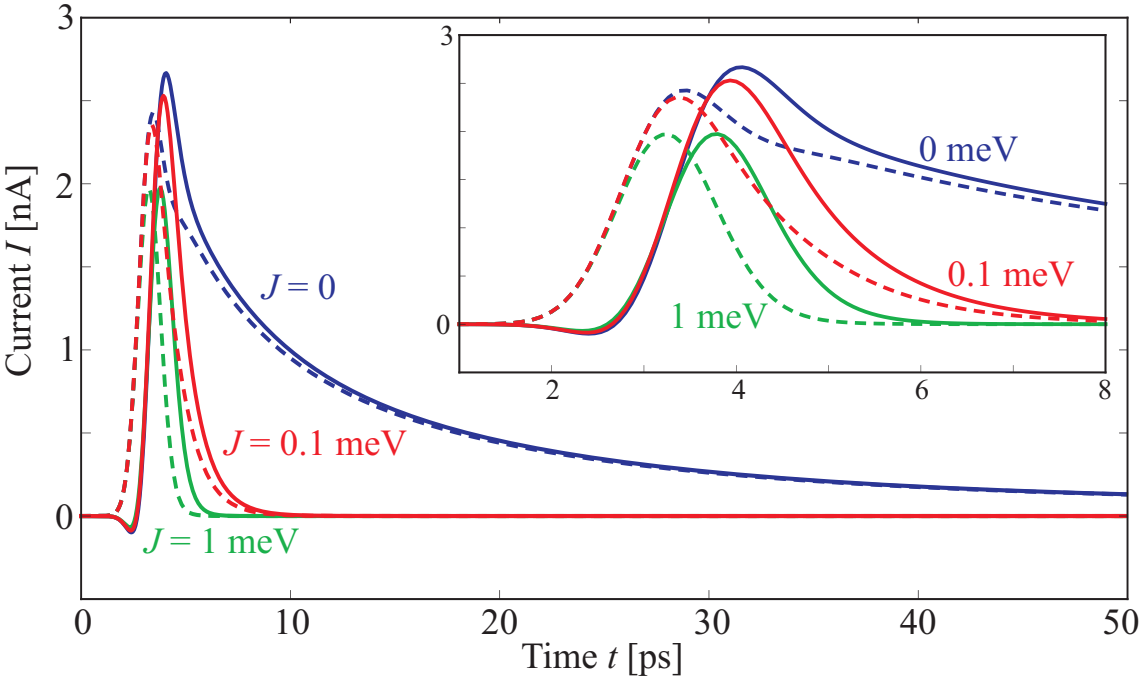

Figure 4.9: Excitation by Gaussian shaped laser pulses with width $\tau_s = 0.5$ ps and field-maximum at 3 ps. Dotted line $-I_L$, solid line I_R. Reduced IVR extend the temporal range of the switch. Incertion shows zoom into temporal range $1 - 8$ ps.

4.4.1 Influence of reduced molecule-lead coupling

Finally we analyze the behavior of optical excited molecule if the molecule-lead coupling is ten times smaller and therefore the electron rests longer in the molecule. Fig. 4.4.1 and Fig. 4.4.1 show the transient current over time. Unfortunately the current switch is degenerated in a way that I_L and $-I_R$ are strongly different at all times. In a first phase the molecule is charged symmetrically from both electrodes, following by a longer time of symmetrically discharge to both electrodes. Such behavior is not suitable for a current switch.
The IVR-strength influences the $I(t)$ curves in a way that longer lifetime of the vibrational excited states result in faster and stronger charging/discharging since more transmission channels are available. The population of the vibrational levels Fig. 4.8 show that it is accumulating in the low vibrational levels, but the transition backwards to the uncharged ground state is quite slow due to the low molecule-lead coupling and the slow transition rate. The inappropriate behavior of current switches with a small molecule lead coupling was already discovered in [12] and is approved by our calculations.

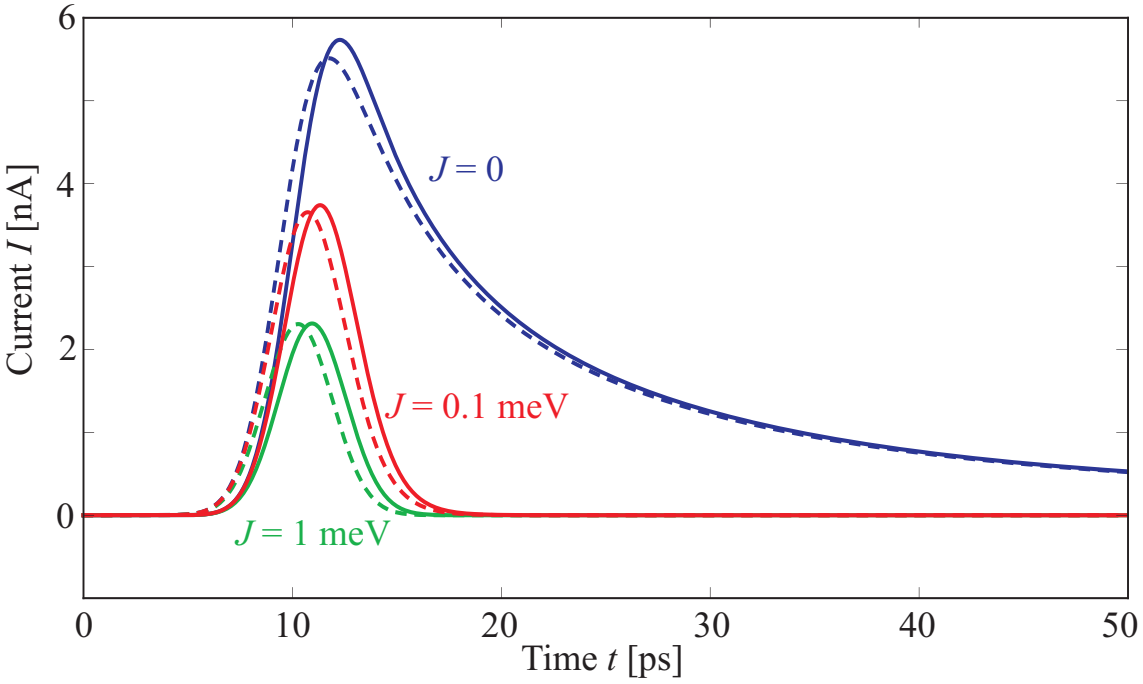

Figure 4.10: Excitation by Gaussian shaped laser pulses with width $\tau_S = 5$ ps and field-maximum at 10 ps. Dotted line $-I_L$, solid line I_R. In contrast to the ultra-short laser pulse no time of charge insertion from both leads is determined.

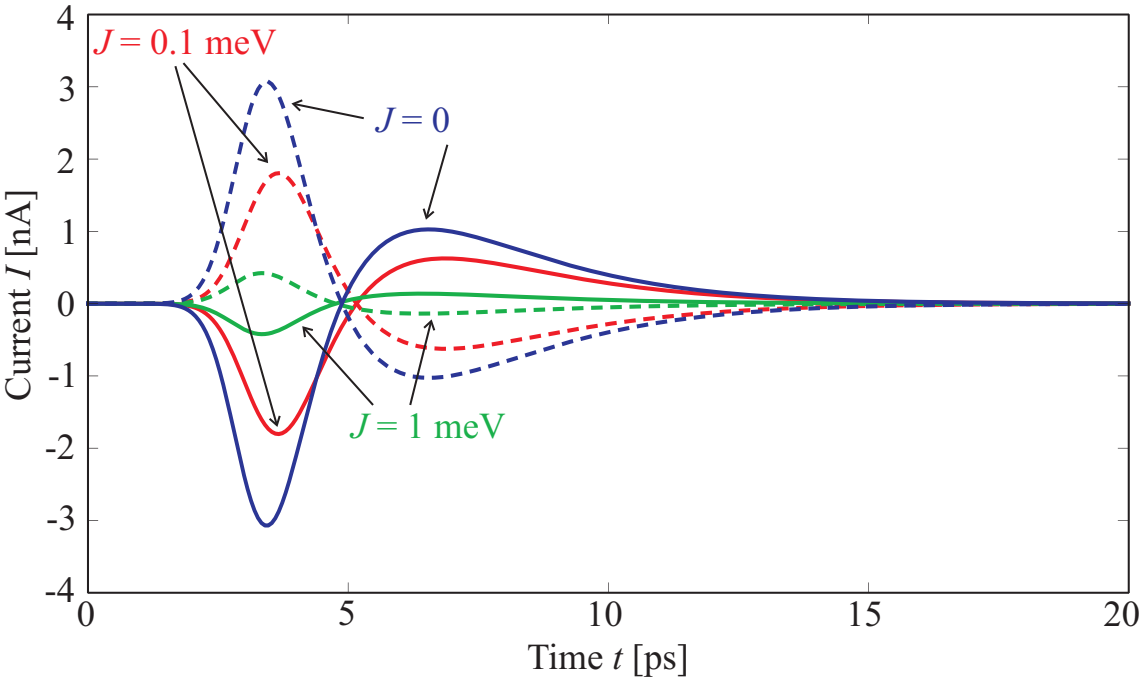

Figure 4.11: Excitation by Gaussian shaped laser pulses with width $\tau_s = 0.5$ ps and field-maximum at 3 ps. Dotted line $-I_L$, solid line I_R. 10 times reduced molecule lead coupling of $\Gamma = 0.1$ meV leads to a degenerated current switch.

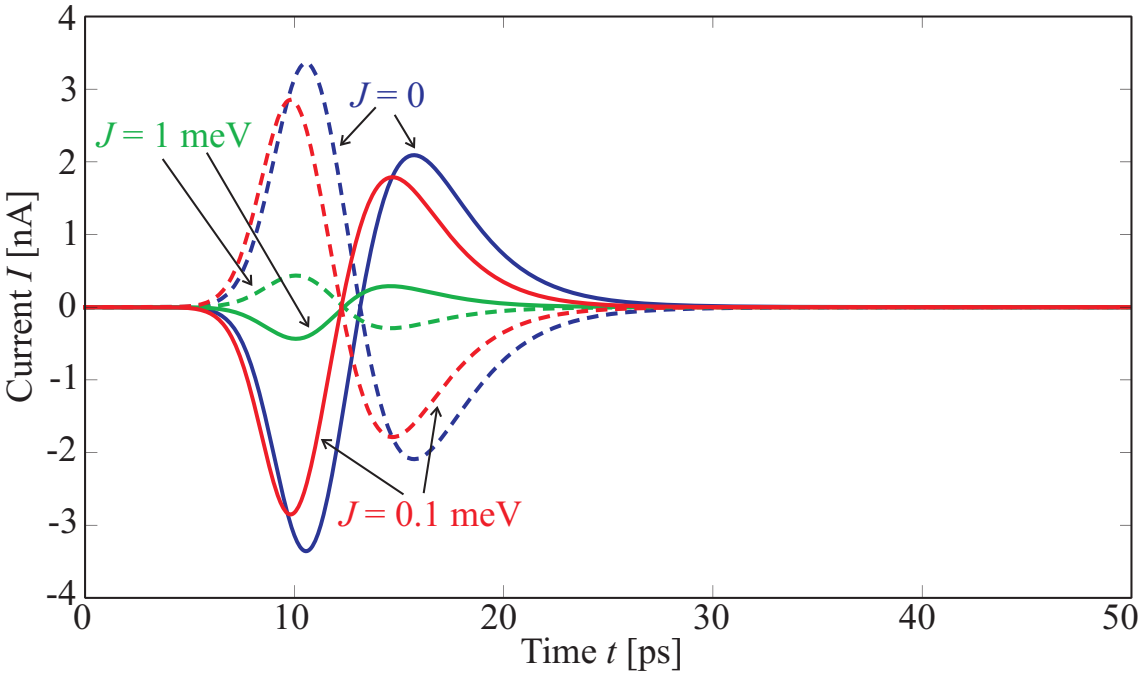

Figure 4.12: Excitation by Gaussian shaped laser pulses with width $\tau_s = 5\,\text{ps}$ and field-maximum at 10 ps. Dotted line $-I_L$, solid line I_R. 10 times reduced molecule lead coupling of $\hbar\Gamma = 0.1\,\text{meV}$ leads to a degenerated current switch.

5. Conclusion

In this thesis the inelastic charge transmission through single molecules attached to nano-electrodes was analyzed theoretically. The density matrix theory based on the equation of motion (EOM) of the molecules reduced density operator was chosen as approach. The resulting EOM were solved numerically. In order to investigate the possibilities of optical switching the interaction with an oscillating external optical field has been included to the EOM.
Firstly the influence of the limitation of the number of vibrational modes on steady state and time-resolved currents was checked. It was shown that a restriction to 20 modes is sufficient for our further purposes. Afterwards the steady state currents for a range of applied voltage have been calculated and the process of charging and discharging including the light-caused was observed. The importance of intramolecular vibrational relaxation (IVR) for potential light-controlled switchs was underlined.
Furthermore the transient currents through molecules excited by laser pulses were observed. It could be shown that current switchs are possible in a voltage range at which molecules are conducting with photoexcitation and isolating without. The reduction of the molecule-lead coupling leads to a degenerated behavior with no usable transient current. Under such conditions optical switching is not possible.
For low values of IVR the formation of a self-stabilized junction was shown. This leads to a slowly decreasing transient current after the laser pulse excitation. This highlights the importance of the formation of vibrational states, especially if they are long-living.

Bibliography

[1] Georg Simon Ohm. *Die galvanische Kette, mathematisch bearbeitet.* T. H. Riemann, 1827.

[2] Florian Klimm. Charge transmission through a single molecule, 2010.

[3] Luxia Wang and Volkhard May. Charge transmission through single molecules: Effects of nonequilibrium molecular vibrations and photoinduced transitions. *Chemical Physics*, May 2010.

[4] Luxia Wang and Volkhard May. External field control of charge transmission through single molecules: Switching effects and transient currents. *Journal of Electroanalytical Chemistry*, 2011.

[5] Tony C. Scott, Monique Aubert-Frécon, and Johannes Grotendorst. New Approach for the Electronic Energies of the Hydrogen Molecular Ion. *Chemical Physics*, http://arxiv.org/abs/physics/0607081v1, 2006.

[6] Volkhard May and Oliver Kühn. *Charge and Energy Transfer Dynamics in Molecular Systems*. Wiley-VCH Verlag, 3. edition, February 2011.

[7] Wichard Beenken. Einführung in die Quantenchemie Kapitel 2: Potentialflächen, 2006.

[8] Franz Schwabel. *Quantenmechanik*, volume 1. Springer, 7. edition, 2007.

[9] Michael Galperin, Abraham Nitzan, and Mark A. Ratner. The non-linear response of molecular junctions: the polaron model revisited. *Journal of Physics: Condensed Matter*, 20(374107), 2008.

[10] John von Neumann. Wahrscheinlichkeitstheoretischer Aufbau der Quantenmechanik. *Göttinger Nachrichten*, 1927.

[11] Günter Mahler and Volker A. Weberruß. *Quantum Networks*. Springer, 2nd, revised and enlarged edition, 2010.

[12] Luxia Wang and Volkhard May. Laser pulse induced transient currents through a single molecule. *Phys. Chem. Chem. Phys.*, 10(1039), 2011.

[13] Peter N. Brown, George D. Byrne, and Alan C. Hindmarsh. VODE, a variable-coefficient ODE solver. *SIAM Journal*, 10(5), September 1989.

[14] Tobias Zentel. Theorie der nichstrahlenden Deaktivierung von Molekülen. *Bachelorarbeit HU Berlin,* September 2010.

[15] Volkhard May and Oliver Kühn. Optical filed control of charge transmission through a molecula wire. i. generalized master equation description. *Physical Review B,* March 2008.

[16] Timm Bredtmann. Quantendynamische Simulationen zur Laserkontrolle von Kernschwingungen: Schwingungsdämpfung in Systemen mit konischer Durchschneidung.

Selbständigkeitserklärung

Hiermit versichere ich, dass ich die vorliegende Arbeit selbständig verfasst habe und keine anderen als die angegebenen Quellen und Hilfsmittel verwendet habe.

Florian Klimm
Berlin, den September 2011